UC San Diego

UC San Diego Electronic Theses and Dissertations

Title

Memory CD8 T cell Fate Divergence in Early Infection

Permalink

https://escholarship.org/uc/item/8q8261k1

Author

Yao, Priscilla

Publication Date

2023

Peer reviewed|Thesis/dissertation

eScholarship.org Powered by the California Digital Library
University of California

UNIVERSITY OF CALIFORNIA SAN DIEGO

Memory CD8 T cell Fate Divergence in Early Infection

A Thesis submitted in partial satisfaction of the requirements
for the degree Master of Science

in

Biology

by

Priscilla Yao

Committee in charge:

Professor John T. Chang, Chair
Professor James T. Kadonaga, Co-Chair
Professor Ella Tour

2023

The Thesis of Priscilla Yao is approved, and it is acceptable in quality and form for publication on microfilm and electronically.

University of California San Diego

2023

TABLE OF CONTENTS

LIST OF FIGURES

LIST OF ABBREVIATIONS

CCR9	C-C motif chemokine receptor 9
CD	Cluster of differentiation
dpi	Days post-infection
GzmA	Granzyme A
iKO	Inducible knock-out
IP	Intraperitoneal
LCMV	Lymphocytic Choriomeningitis Virus
LPAM-1	Lymphocyte Peyer's patch adhesion molecule-1 [Integrin $\alpha4\beta7$]
Ly6C	Lymphocyte antigen 6 complex
mLN	Mesenteric lymph node
PBS	Phosphate buffered saline
PFU	Plaque-forming units
RO	Retro-orbital
scRNA-seq	Single-cell RNA sequencing
SEM	Standard error of the mean
siIEL	Small intestine intra-epithelial layer
TCF1/7	T cell factor 1/7
T_{CIRCM}	Circulating memory
T_{CM}	Central memory
TCR	T cell receptor
T_{EM}	Effector memory

T_{RM}	Tissue-resident memory
t-T_{EM}	Terminal effector memory
WT	Wildtype

ACKNOWLEDGEMENTS

The accomplishment of this project would have been extremely difficult without all the help and support from the mentors of my lab – John Chang, Paul Hsu, and Elena Lin. More importantly, this project was only made possible with the help of my research partner, Emily Liu.

I am immensely grateful to my family, instructors, and professors who have expressed their belief in my capabilities in times of self-doubt. Their support has equipped me with strength to overcome countless obstacles throughout my journey as a student and as a researcher.

Lastly, without my prior mentor – Tiani Louis, I would not have been presented with the privilege to join the Chang Lab and acquire the skills beneficial to my future endeavors.

ABSTRACT OF THE THESIS

Memory CD8 T cell Fate Divergence in Early Infection

by

Priscilla Yao

Master of Science in Biology

University of California San Diego, 2023

Professor John T. Chang, Chair
Professor James T. Kadonaga, Co-Chair

Tissue-resident memory (T_{RM}) $CD8^+$ T cells are a non-circulating subset of memory T cells that reside within barrier tissues and provide rapid and sustained host defense against reinfections. Recent studies have revealed that the location at which T cells are activated influences their trafficking patterns and cell fates. However, these findings often investigate T cells following memory formation, whereby the time and location of memory T cell fate

divergence is not well characterized. By analyzing $CD8^+$ T cells in the spleen, mesenteric lymph nodes, and small intestines using flow cytometry, I showed that the mesenteric lymph node exhibited a $CCR9^{hi}$ $CD62L^{lo}$ and a $CD62L^{hi}$ $CCR9^{lo}$ population, with the former bearing phenotypic resemblance to bona fide gut-T_{RM} cells and the latter to circulating memory T cells at 4 days post-infection. These findings suggest that memory T cells begin to specify their cell fates in the draining lymph node during early infection, prior to tissue entry. Additionally, I showed that the transcription factor TCF1, known to promote circulating memory T cell differentiation, is required for the formation of all memory precursors. These findings provide additional insight toward our understanding of the early signals that influence $CD8^+$ T cell fate specification, serving as plausible treatments to tissue-specific or systemic infections.

INTRODUCTION

$CD8^+$ T cells are members of the adaptive immune response critical for host defense against pathogens. In response to a microbial infection, naïve $CD8^+$ T cells residing in secondary lymphoid organs, such as the spleen and lymph nodes, become activated and undergo asymmetrical cell division into distinct effector and memory subsets[1]. Short-lived effector $CD8^+$ T cells provide acute control of pathogens via secretion of pro-inflammatory cytokines and cytolytic granules that kill infected cells, while long-lived memory $CD8^+$ T cells can rapidly reactivate upon reinfection thus providing sustained host defense. Memory $CD8^+$ T cells exhibit heterogeneity and are broadly classified as either circulating or non-circulating[2]. Circulating memory (T_{CIRCM}) cells are further subdivided into central memory (T_{CM}), effector memory (T_{EM}), and terminal effector memory (t-T_{EM}) according to their trafficking patterns as well as their phenotypic and functional properties[3, 4]. Tissue-resident memory (T_{RM}) cells are non-circulating and are widely distributed across various tissues and barrier surfaces of the body[3], providing rapid pathogen clearance upon reinfection. However, dysregulated T_{RM} cells are involved in the pathogenesis of various autoimmune and chronic inflammatory diseases[5, 6]. Thus, understanding the mechanisms that drive T_{RM} formation and maintenance would provide further insight toward vaccine immunogenicity[7], cancer immunotherapy[6, 7], and immunopathology[10].

Although the key regulators that promote the differentiation of T_{CIRCM} and T_{RM} cells have been studied in greater depth[11], the timing and location at which these cell fates diverge are yet to be elucidated. More specifically, it remains uncertain whether T_{CIRCM} and T_{RM} cell fates diverge prior to or post tissue entry. Initially, it has been demonstrated that $CD8^+$ T cells may be influenced by the inflamed tissue microenvironment to favor T_{RM} differentiation[12], but a T_{RM}-like transcriptional signature has been identified within the effector T cell pool in the peripheral

blood, prior to tissue entry in studies of skin infection[13]. These previous findings have prompted our lab to investigate the bifurcation in T_{RM} and T_{CIRCM} cell fates in the context of the gut. More specifically, it remains unclear whether this bifurcation occurs while T cells are undergoing proliferation in the secondary lymphoid organs (spleen or mesenteric lymph node (mLN)), or after they reach the small intestines. Therefore, our lab has analyzed $CD8^+$ T cells from the spleen, mLN, and small intestine intra-epithelial layer (siIEL) at 4, 7, and 30 days post-infection (dpi) using single-cell RNA-sequencing (scRNA-seq). The selected timepoints reflect early infection, peak of infection, and post memory cell formation in our infection model. Unbiased clustering revealed two transcriptionally distinct populations in the mLN starting at 4 dpi. One of the two populations exhibit a gene signature reminiscent of bona fide siIEL-T_{RM} cells, which express high *Ccr9*, *Id2, Gzma,* and *Prdm1*[11, 14]. The other population exhibits a gene signature reminiscent of bona fide T_{CIRCM} cells, which express high *Id3, Tcf7,* and *Sell*[11]. On the basis of this data, we hypothesized there are putative precursors to T_{RM} and T_{CIRCM} cells present in the mLN at 4 dpi, prior to T cell entry into the small intestines.

To test this hypothesis, I used flow cytometry to analyze $CD8^+$ T cells from the spleen, mLN, and siIEL at 4 and 5 dpi. The results reveal that putative siIEL-T_{RM} and T_{CIRCM} precursors are present in the mLN starting at 4 dpi, indicating that the bifurcation in T_{RM} and T_{CIRCM} cell fates occur in the draining lymph node, prior to tissue entry. Additionally, I performed an inducible deletion of *Tcf7*, previously known to promote T_{CIRCM} differentiation, to validate the role it plays in skewing memory T cell fate specification. Unexpectedly, the results reveal that *Tcf7* is essential for the formation of both T_{CIRCM} and T_{RM} precursors.

MATERIAL & METHODS

Mice

All mice were housed in an American Association of Laboratory Animal Care-approved facility at the University of California, San Diego (UCSD). Experiments were conducted in accordance with protocols approved by the UCSD Institutional Animal Care and Use Committee. C57BL/6J (CD45.2) and B6.SJL-*Ptprc*^{a}*Pepc*^{b}*/BoyJ* (CD45.1) mice were purchased from the Jackson Laboratory. *Tcf7*$^{fl/fl}$ and *Ert2*-Cre^{+} mice were purchased from Jackson Laboratory and bred together with P14 T-cell receptor (TCR) transgenic mice to generate *Tcf7*$^{fl/fl}$*Ert2*-Cre^{+} (TCF1 iKO) P14 mice. Donor mice were P14^{+}, while recipient mice were P14^{-}. P14 mice exhibit a transgenic TCR that recognizes the Lymphocytic Choriomeningitis Virus (LCMV) peptide residues 33-41. Thus, a LCMV infection will induce a controlled T cell response in the donor P14 CD8^{+} T cells within recipient mice. All mice were used between 6-9 weeks of age.

Adoptive transfer and infection

Donor CD45.1^{+}, CD45.1.2^{+}, or CD45.2^{+} CD8^{+} P14 T cells were adoptively transferred into congenically distinct CD45.1^{+} or CD45.2^{+} recipient mice (2.5 x 10^{5} or 5 x 10^{5} cells/mouse) by retroorbital (RO) injection. Donor cells and recipient cells that express different congenic markers (CD45.1 vs. CD45.1.2) were used to distinguish the different cell populations within the same mouse by flow cytometry analysis. In competition experiments, TCF1 iKO CD8^{+} P14 T cells (2.5 x 10^{5} cells/mouse) were co-transferred with control (wildtype) CD8^{+} P14 T cells (2.5 x 10^{5} cells/mouse). An aliquot of the 1:1 co-transfer cell suspension was sampled using a flow cytometer to correct for the input ratios between wildtype CD8^{+} P14 T cells vs. TCF1 iKO CD8^{+} P14 T cells. Recipient mice were infected via intraperitoneal (IP) injection with 2 x 10^{5} plaque-

forming units (PFU) of LCMV-Armstrong 20 minutes following adoptive transfer of donor cells. Infection by LCMV-Armstrong will result in an acute systemic infection, with pathogen clearance observed at 8-10 days post-infection.

Tamoxifen Treatment

For the inducible deletion of *Tcf7*, tamoxifen was administered by IP injection (1 mg/mouse x 5 days). A 100 mg/mL tamoxifen stock solution was made using 100% ethanol, which is further diluted at 1:10 in 100% sunflower seed oil. Each mouse received 100μL of tamoxifen treatment per day for 5 days.

Lymphocyte isolation

To preserve $CD8^+$ T cells during their isolation process, Treg-Protector (Biolegend) was administered according to manufacturer's recommendation by IP injection to mice 15 minutes prior to sacrifice. The spleen, mLN and small intestines were harvested upon sacrifice. For lymphocyte isolation in the spleen and mLN, the tissues were passed through a 70μm strainer to establish a single cell suspension. The spleen was further treated with Red Blood Cell Lysing Buffer Hybri-Max (Sigma) to exclude erythrocytes. For lymphocyte isolation from the small intestine, Peyer's patches were excised and the tissue was cut longitudinally for rinsing in PBS. To extract lymphocytes from the siIEL, the tissues were cut into 1 cm pieces and shaken in DTE buffer [dithioerythritol (1μg/ml; Thermo Fisher Scientific) in 10% HBSS and 10% HEPES bicarbonate] at 37°C for 30 minutes. The supernatant containing the siIEL cells were collected and centrifuged. The remaining pellet was resuspended and placed in a 44%/67% Percoll gradient for lymphocyte isolation upon centrifugation. The siIEL lymphocytes were collected between the density gradient.

Flow cytometry and antibodies

To assess the extracellular and intracellular proteins expressed by $CD8^+$ T cells, fluorescent antibodies targeting specific proteins were used. All cellular staining and treatment was performed shielded from light. Single-cell suspensions of spleen, mLN, and siIEL samples were first stained with a Fixable Viability Dye eFluor780 (Thermo Fisher Scientific) at 1:1000 for 10 minutes on ice. Cells were further stained with the following fluorescent cell-surface antibodies from Biolegend at 1:100 for 30 minutes on ice: CCR9 (CW-1.2), CD45.1 (A20), CD45.2 (104), CD62L (MEL-14), LPAM-1 (DATK32), Ly6C (HK1.4). For intracellular staining, cells were fixed for 30 minutes at room temperature and permeabilized using the Foxp3/Transcription Factor Staining Buffer Set (Thermo Fisher Scientific). Post fixation, cells were stained in permeabilization buffer for 30 minutes at room temperature with the following intracellular antibodies diluted at 1:50: T-bet [4B10 (Biolegend)], TCF1 [S33-966 (BD Biosciences)], GzmA [GzA-3G8.5 (Thermo Fisher)]. Cells were resuspended in PBS for flow cytometry analysis.

Flow cytometry analysis

Flow cytometry was performed by running samples on a Novocyte 3000 (Agilent) and data was collected using the NovoExpress (Agilent) software. Analysis of flow cytometry data was performed using the FlowJo software (BD Biosciences). Statistical analyses of flow cytometry data were analyzed using the Prism (GraphPad) software. Statistical parameters and tests performed are as indicated in the figure legends.

RESULTS

Putative siIEL-T_{RM} and T_{CIRCM} precursors can be identified in the mLN at 4 days post-infection

Previously, our laboratory performed a scRNA-seq analysis, which identified a siIEL-T_{RM}-like population expressing high *Ccr9* and a T_{CIRCM}-like population expressing high *Sell* in the mLN at 4 dpi. Since T cells require the expression of a tissue-homing marker to facilitate its migration, high expression of C-C motif chemokine receptor 9 (CCR9) induces migration to the gut, while expression of CD62L (encoded by *Sell*) induces migration to the lymph nodes. Therefore, we hypothesized that a $CD8^+$ T cell population expressing $CCR9^{hi}$ $CD62L^{lo}$ (denoted as $CCR9^{hi}$) contained putative siIEL-T_{RM} precursors, whereas a population expressing $CD62L^{hi}$ $CCR9^{lo}$ (denoted as $CD62L^{hi}$) contained putative T_{CIRCM} precursors. Moreover, we predict that the mLN population expressing $CCR9^{lo}$ $CD62L^{lo}$ potentially contain short-lived effector cells, since this population is neither gut-homing nor lymph node homing.

To phenotypically validate the scRNA-seq analysis performed by our laboratory, I adoptively transferred wildtype P14 $CD8^+$ T cells into congenically distinct recipients, which were subsequently infected with Lymphocytic Choriomeningitis Virus (LCMV) and sacrificed at 4 and 5 dpi (**Figure 1A**). P14 $CD8^+$ T cells exhibit transgenic T cell receptors that recognize the LCMV peptide residues 33-41. Thus, infecting recipient mice with LCMV, promotes activation and proliferation of the donor P14 $CD8^+$ T cells. At 4 and 5 dpi, I identified the putative siIEL-T_{RM} and T_{CIRCM} precursors (donor P14 $CD8^+$ T cells) by their respective expression of CCR9 and CD62L in the mLN (**Figure 1B**). I then analyzed the expression of phenotypic markers α4β7, T-bet, GzmA, Ly6C, and TCF1 in putative siIEL-T_{RM} ($CCR9^{hi}$) and T_{CIRCM} precursors ($CD62L^{hi}$) in the mLN at 4 dpi.

The expression of integrin α4β7 [shown as LPAM-1] enables $CD8^+$ T cells to integrate and adhere to the siIEL[15]. At 4 and 5 dpi, $CCR9^{hi}$ cells expressed higher concentrations of α4β7 relative to $CD62L^{hi}$ cells (**Figure 1C**). The expression of α4β7 also increased from 4 to 5 dpi in both $CCR9^{hi}$ and $CD62L^{hi}$ cells. Since CCR9 and α4β7 are well-established molecules that mediate trafficking and adhesion to the intestinal epithelium[15], we concluded that $CD8^+$ T cells expressing high levels of these molecules were likely to give rise to siIEL-T_{RM} cells.

The T-box transcription factor, T-bet, is known to be abundantly expressed in both short-lived effector and effector memory $CD8^+$ T cells, but is minimally expressed by mature T_{RM} cells[16, 17]. At 4 and 5 dpi, $CCR9^{hi}$ cells exhibited higher expression of T-bet relative to $CD62L^{hi}$ cells (**Figure 1D**). Moreover, the expression of T-bet increased from 4 to 5 dpi in both $CCR9^{hi}$ and $CD62L^{hi}$ cells.

Granzymes are cytolytic granules secreted by $CD8^+$ T cells onto infected cells to reduce pathogen spread by inducing apoptosis. At 4 and 5 dpi, granzyme A (GzmA) expression trended higher in $CCR9^{hi}$ cells relative to $CD62L^{hi}$ cells (**Figure 1E**). GzmA appears to be expressed at similar levels in both $CCR9^{hi}$ and $CD62L^{hi}$ cells between 4 and 5 dpi. These results suggest that $CCR9^{hi}$ cells may be putative siIEL-T_{RM} precursors, as T_{RM} cells have been reported to express higher levels of GzmA relative to T_{CM} cells, a population of T_{CIRCM} cells[14].

Lymphocyte antigen 6 complex (Ly6C) is a lymphoid homing glycoprotein highly expressed by T_{CM} cells[18]. The expression of Ly6C is greater in the $CD62L^{hi}$ cells relative to $CCR9^{hi}$ cells at 4 and 5 dpi (**Figure 1F**). The expression of Ly6C increases from 4 to 5 dpi in both $CCR9^{hi}$ and $CD62L^{hi}$ cells. These findings suggest that $CD62L^{hi}$ cells exhibit a Ly6C phenotype similar to that of T_{CM} cells, which are a subset of T_{CIRCM} cells.

T cell factor 1 (TCF1, encoded by *Tcf7*) is a transcription factor essential for T_{CIRCM} differentiation[19] and is highly expressed in T_{CM} cells[20]. At 4 and 5 dpi, $CD62L^{hi}$ cells expressed higher levels of TCF1 relative to $CCR9^{hi}$ cells (**Figure 1G**). Additionally, there is reduced expression of TCF1 from 4 to 5 dpi in both $CCR9^{hi}$ and $CD62L^{hi}$ cells.

Overall, putative siIEL-T_{RM} precursors defined by $CCR9^{hi}$ $CD62L^{lo}$ exhibited an increased expression of α4β7, T-bet, and GzmA relative to putative T_{CIRCM} cells. Putative T_{CIRCM} precursors defined by $CD62L^{hi}$ $CCR9^{lo}$ exhibited an increased expression of Ly6C and TCF1 relative to putative siIEL-T_{RM} precursors.

Figure 1. Putative siIEL-T_{RM} and T_{CIRCM} precursors can be identified in the mLN at 4 days post-infection

(A) Experimental setup. Donor wildtype P14 $CD8^+$ T cells were adoptively transferred into recipient mice by RO injection. Recipients were subsequently infected with LCMV-Armstrong by IP injection. Spleen, mLN, and siIEL were harvested at 4 and 5 dpi.

(B) A representative flow cytometry plot depicting the expression of CCR9 by CD62L in donor wildtype P14 $CD8^+$ T cells isolated from the mLN.

(C-G) Representative flow cytometry plots (left) and bar plots (right) depicting frequencies of wildtype P14 $CD8^+$ T cells expressing (C) α4β7 (D) T-bet (E) GzmA (F) Ly6C (G) TCF1 in the mLN gated on $CCR9^{hi}$ $CD62L^{lo}$ and $CD62L^{hi}$ $CCR9^{lo}$ populations as shown in (B). A biologic negative control was utilized to set the LPAM-1^+, T-bet^+, and $GzmA^+$ gate. An isotype negative staining control was utilized to set the $Ly6C^+$ gate. A biologic positive control was utilized to set the $TCF1^+$ gate.

Data depicted in the bar graphs are represented as mean ± SEM. Multiple paired t tests were performed. *$p < 0.05$, **$p < 0.01$, ***$p < 0.001$, ****$p < 0.0001$. Data are representative of ≥ 2 independent experiments, with 6 mice per experiment. (E-G) A distinct dataset, in which 3 mLN were stained with one antibody cocktail and the remaining 3 were stained with a separate antibody cocktail.

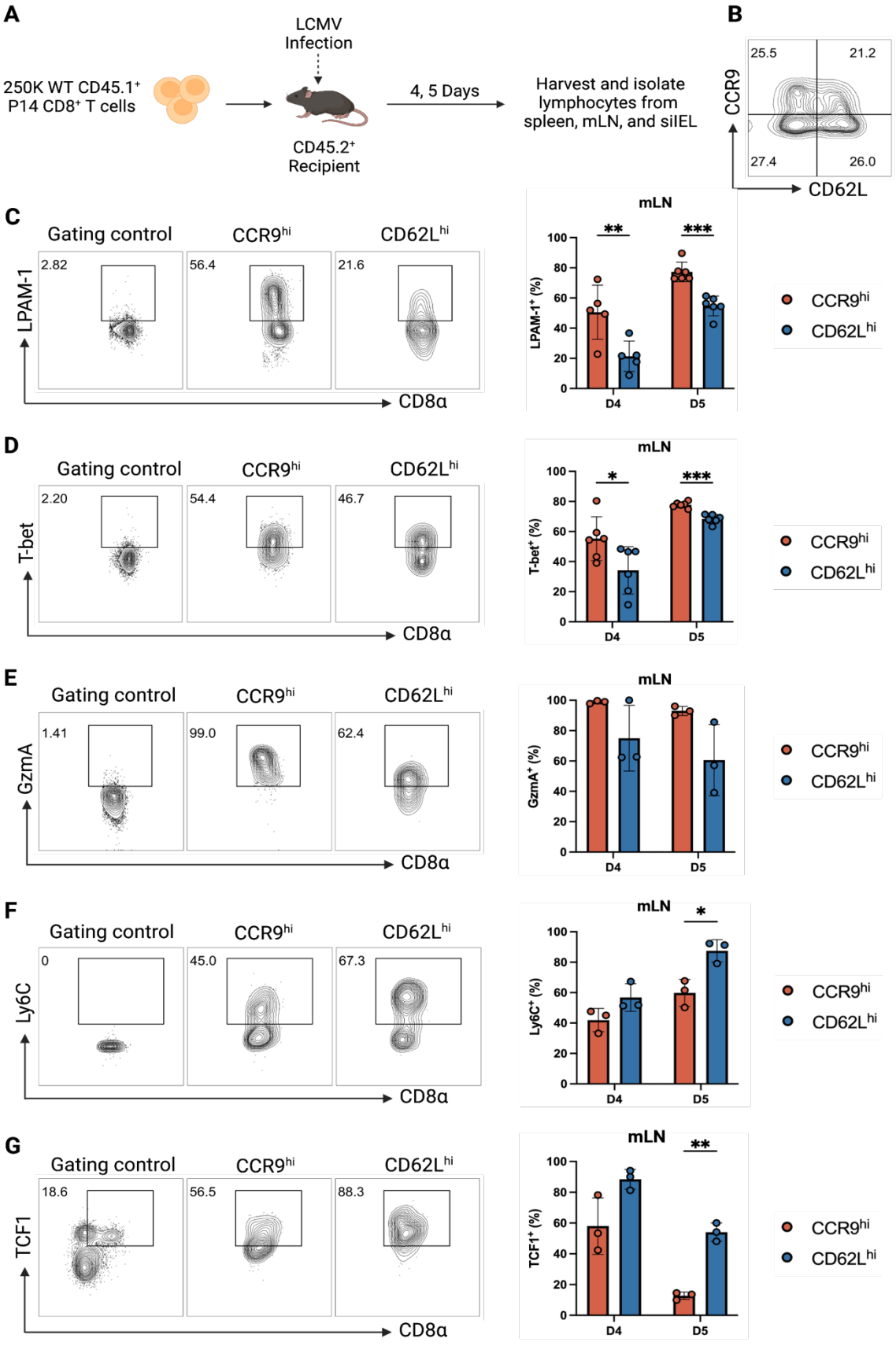
A
LCMV Infection
250K WT CD45.1+ P14 CD8+ T cells
4, 5 Days
CD45.2+ Recipient
Harvest and isolate lymphocytes from spleen, mLN, and siIEL
B
CCR9
CD62L
25.5
21.2
27.4
26.0
C
Gating control
CCR9hi
CD62Lhi
LPAM-1
CD8α
2.82
56.4
21.6
mLN
LPAM-1+ (%)
D4
D5
CCR9hi
CD62Lhi
D
T-bet
2.20
54.4
46.7
T-bet+ (%)
E
GzmA
1.41
99.0
62.4
GzmA+ (%)
F
Ly6C
0
45.0
67.3
Ly6C+ (%)
G
TCF1
18.6
56.5
88.3
TCF1+ (%)

Tcf7 is required for the formation of both putative T_{CIRCM} and T_{RM} precursors

Previous studies have established that the formation and maintenance of T_{CM} cells, a subset of T_{CIRCM} cells[20], requires the transcription factor TCF1 (encoded by *Tcf7*). Since TCF1 has been well documented to be required for T_{CIRCM} differentiation and has been shown to suppress lung T_{RM} development[21], we hypothesized that the deletion of TCF1/7 would result in a numerical deficit of $CD62L^{hi}$ putative T_{CIRCM} precursors, with an increase in $CCR9^{hi}$ T_{RM} precursors. Moreover, we reasoned that TCF1/7 deletion may increase putative T_{RM} precursors because TCF1 has been reported to antagonize the expression of Blimp1 (encoded by *Prdm1*) an essential transcription factor promoting T_{RM} differentiation[22]. To determine whether *Tcf7* is critical for the formation of putative T_{CIRCM} precursors, we used a $Tcf7^{fl/fl}$ ER-Cre inducible knockout (iKO) mouse model. $Tcf7^{fl/fl}$ ER-Cre P14 donor mice were treated with tamoxifen for 5 consecutive days prior to adoptive transfer to delete *Tcf7* (**Figure 2A**).

To directly assess the impact of a TCF1/7 deletion relative to the wildtype (WT) on the formation of putative memory precursor cells in the same mouse at 4 and 5 dpi, I adoptively transferred a 1:1 mixture of WT and TCF1/7 iKO P14 $CD8^+$ T cells into recipients that were subsequently infected with LCMV (**Figure 2A**). The deletion of TCF1/7 resulted in a numerical reduction of donor $CD8^+$ T cells across the spleen, mLN, and siIEL (**Figure 2B**). At 4 dpi, the effect of TCF1/7 deletion was not apparent in the spleen; however, there was a greater reduction in total $CD8^+$ T cells across all three tissues by 5 dpi.

To determine if the reduction in total donor $CD8^+$ T cells upon TCF1/7 deletion was a reflection of a loss in putative T_{CIRCM} precursors ($CD62L^{hi}$) and not T_{RM} precursors ($CCR9^{hi}$), the proportion of donor $CD8^+$ T cells solely expressing either CCR9 or CD62L was determined across the three tissues at 5 dpi (**Figure 2C**). Analysis of 5 dpi is shown, since the phenotypic

defect is most evident at 5 dpi. Contrary to what was hypothesized, the loss of TCF1/7 resulted in a reduction in both T_{CIRCM} and T_{RM} precursors relative to the WT control. These results suggest that TCF1/7 is essential for the formation of both putative T_{CIRCM} and T_{RM} precursors.

Figure 2. *Tcf7* is required for the formation of both putative T_{CIRCM} and T_{RM} precursors

(A) Experimental setup. Donor *Tcf7*$^{fl/fl}$ ER-Cre mice received tamoxifen treatment by IP injection once per day for 5 consecutive days prior to adoptive transfer into recipient mice. CD8$^+$ T cells from control (WT) and *Tcf7*$^{fl/fl}$ ER-Cre (TCF1/7 iKO) P14 mice were adoptively co-transferred at a 1:1 ratio into 6 recipient mice retro-orbitally per timepoint. Recipient mice were subsequently infected with LCMV-Armstrong by IP injection. Spleen, mLN, and siIEL were harvested at 4 and 5 dpi.

(B) A representative flow cytometry plot (left) of donor WT and TCF1 iKO P14 CD8$^+$ T cells isolated from a recipient mouse, quantified by absolute numbers (top) and proportions (bottom).

(C) Representative flow cytometry plots (left) and bar graphs (right) depicting frequencies of control vs. TCF1 iKO P14 CD8$^+$ T cells expressing CCR9 and CD62L across the three harvested tissues at 5 dpi.

Data depicted in the bar graphs are represented as mean ± SEM. Multiple paired t tests were performed. *$p < 0.05$, **$p < 0.01$, ***$p < 0.001$, ****$p < 0.0001$. Data are representative of ≥ 2 independent experiments, with 6 mice per experiment.

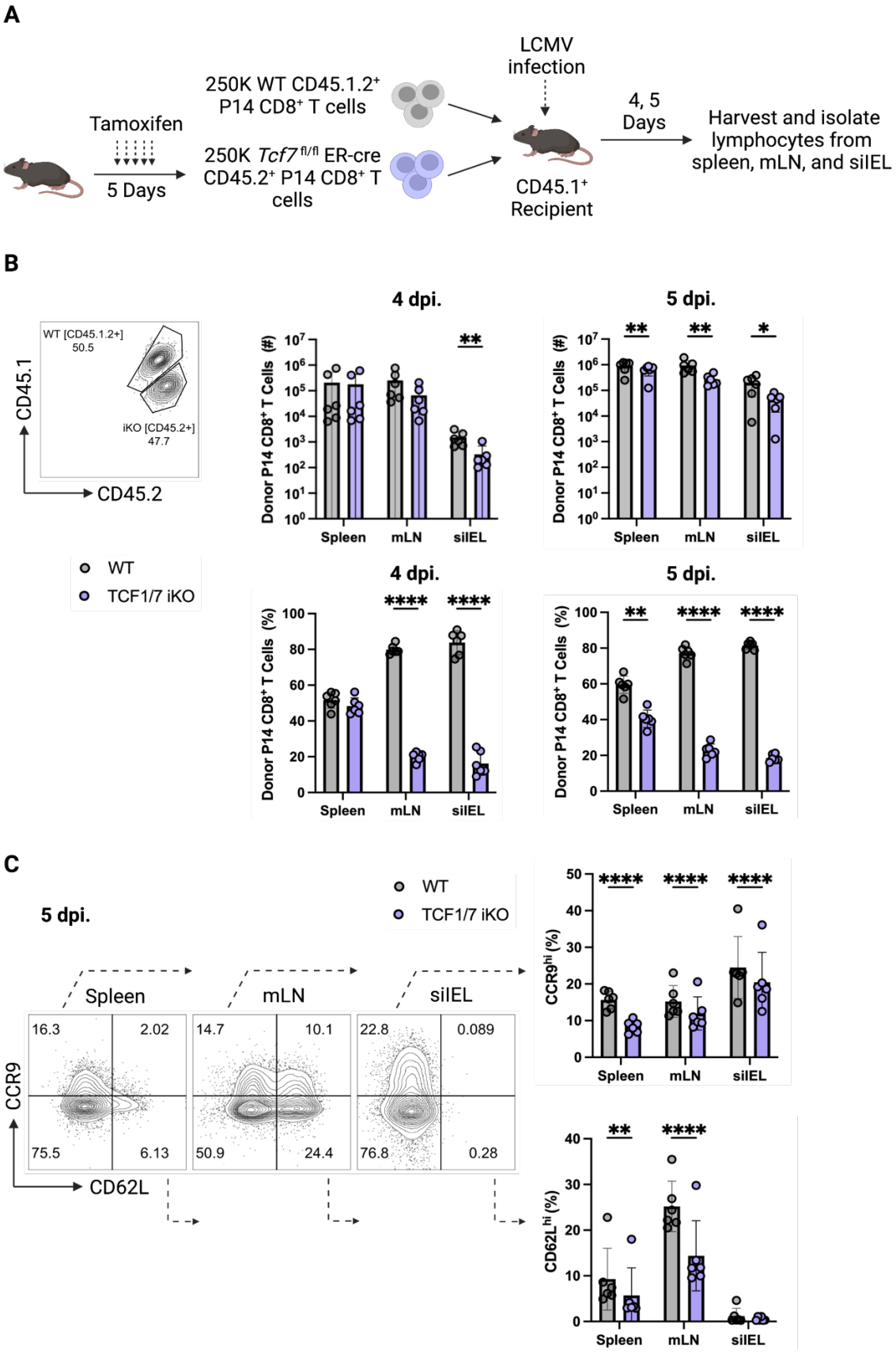
A
Tamoxifen
5 Days
250K WT CD45.1.2+ P14 CD8+ T cells
250K Tcf7 fl/fl ER-cre CD45.2+ P14 CD8+ T cells
LCMV infection
CD45.1+ Recipient
4, 5 Days
Harvest and isolate lymphocytes from spleen, mLN, and siIEL
B
WT [CD45.1.2+] 50.5
iKO [CD45.2+] 47.7
CD45.1
CD45.2
WT
TCF1/7 iKO
4 dpi.
5 dpi.
Donor P14 CD8+ T Cells (#)
Donor P14 CD8+ T Cells (%)
Spleen
mLN
siIEL
C
5 dpi.
WT
TCF1/7 iKO
Spleen
mLN
siIEL
CCR9
CD62L
16.3
2.02
75.5
6.13
14.7
10.1
50.9
24.4
22.8
0.089
76.8
0.28
CCR9hi (%)
CD62Lhi (%)

Overall, these results suggest a model in which $CD8^+$ T cells primed in the mLN undergo proliferation to give rise to several intermediate states of differentiation: (1) short-lived effector cells that will undergo apoptosis after pathogen clearance; (2) precursors to T_{CIRCM} cells that will remain in the circulation; and (3) precursors to siIEL-T_{RM} cells that will migrate to the gut and remain in the epithelium for rapid pathogen clearance upon reinfection (**Figure 3**). The presence of two phenotypically distinct populations in the mLN that each resemble mature T_{RM} and T_{CIRCM} cells, indicate that these two cell fates begin to diverge prior to $CD8^+$ T cells entering the siIEL (**Figure 3**). Moreover, *Tcf7* is not only essential for the differentiation of T_{CIRCM} cells, but it is also critical for the formation of both putative T_{RM} and T_{CIRCM} precursors (**Figure 2**).

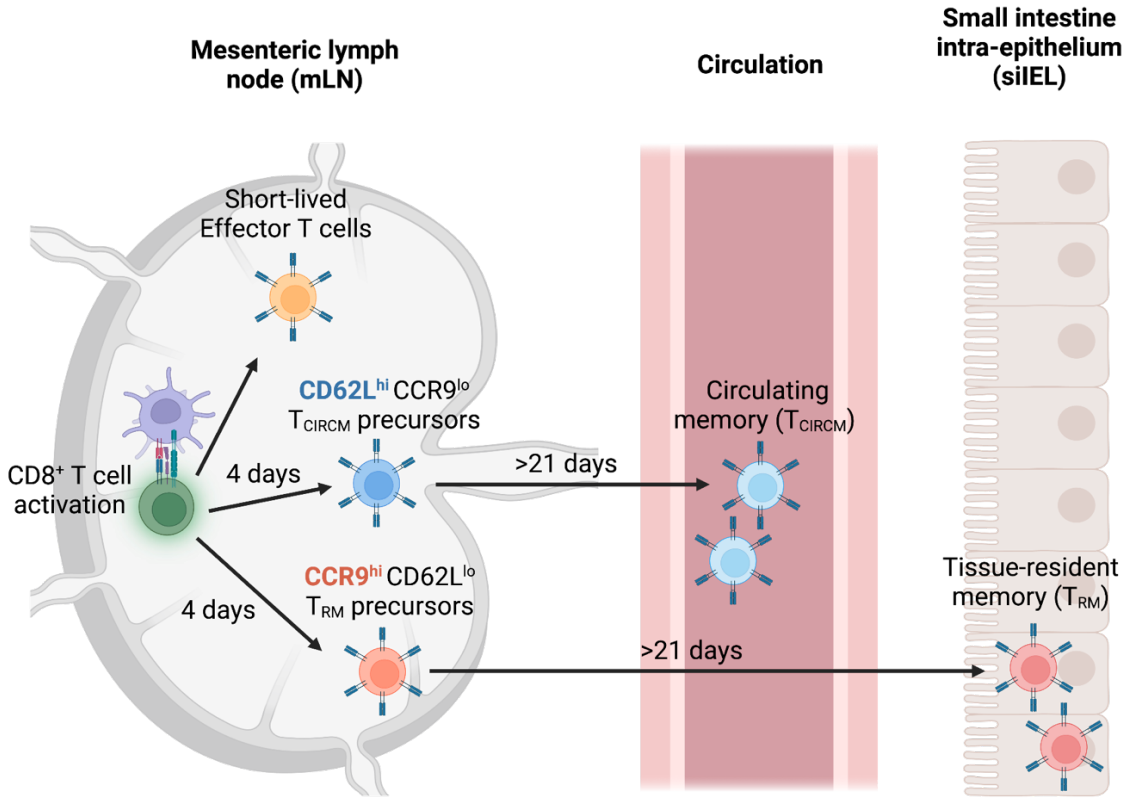

Figure 3. Divergence of CD8$^+$ T_{CIRCM} and T_{RM} cells occur in the mLN at 4 dpi, prior to entry into the siIEL

Representation of the proposed fate divergence model. Model depicts the activation of a naïve CD8$^+$ T cell by an antigen presenting cell, and the activated CD8$^+$ T cell gives rise to heterogenous progeny. At 4 dpi, putative T_{CIRCM} and T_{RM} precursors are observed in the mLN. Upon the formation of memory T cells (>21 dpi), the precursors are predicted to give rise to their respective T_{CIRCM} and siIEL-T_{RM} cells.

DISCUSSION

In similar studies of the gut, the location at which a T cell is activated or primed, influences its trafficking patterns and its subsequent differentiation into T_{RM} and T_{CIRCM} cells[23]. However, it is uncertain whether activated $CD8^+$ T cells experience a divergence in memory T cell fates prior to or post-tissue entry. Here, I demonstrate that starting at 4 dpi, $CD8^+$ T cells in the mLN exhibit two phenotypically distinct populations. One population expresses $CCR9^{hi}$ $CD62L^{lo}$, resembling mature siIEL-T_{RM} cells, while the other population expresses $CD62L^{hi}$ $CCR9^{lo}$, resembling mature T_{CIRCM} cells. Detection of such putative precursor populations imply that some $CD8^+$ T cells are poised to become a specified cell fate prior to entering the tissue, as soon as 4 days post-infection. Both putative siIEL-T_{RM} and T_{CIRCM} precursor populations exhibit functional and phenotypic differences on the basis of α4β7, GzmA, Ly6C, and TCF1 expression, which are in congruence with their putative cell fates. Additional fate-mapping experiments would be required to validate whether $CCR9^{hi}$ $CD62L^{lo}$ and $CD62L^{hi}$ $CCR9^{lo}$ expressing cells would differentiate into siIEL-T_{RM} and T_{CIRCM} cells, respectively.

Although T-bet expression was observed to be greater in putative siIEL-T_{RM} precursor cells and high T-bet expression has been reported to inhibit T_{RM} differentiation[12, 23], these findings remain consistent with reported observations. Notably, high T-bet expression is required during early generation of T_{RM} precursors, but low expression is required in mature T_{RM} cells[12, 23].

Moreover, we hypothesized that TCF1 would only be required for the formation of putative T_{CIRCM} precursors, but not for T_{RM} precursors. However, the results indicate that TCF1 is an important transcriptional regulator in the development of both putative T_{RM} and T_{CIRCM} precursors. TCF1 may potentially regulate memory precursor development on the basis of

promoting proliferation, cell survival, or inhibiting apoptosis. The mechanistic role of TCF1 regulation would require further study with proliferation and apoptotic assays performed on control vs. TCF1/7 iKO $CD8^+$ T cells.

Ultimately, the identification of putative T_{RM} and T_{CIRCM} precursors in the draining lymph node as early as 4 dpi, indicates that the bifurcation in memory cell fates occur prior to $CD8^+$ T cells seeding a target tissue. These findings contribute to the field's understanding of early T cell fate specification and enables us to further explore the roles of other transcriptional regulators that may preferentially promote the formation of tissue-specific or systemic T cell populations. The ability to instruct preferential formation of a specified T cell subset serves as a powerful treatment that may be tailored to combat a specified pathogen. Furthermore, identifying key transcription factors and the regulatory role they play in $CD8^+$ T cell differentiation is also an essential consideration in designing treatments against pathologies surrounding dysregulated T cells.

REFERENCES

1. Chang JT, Palanivel VR, Kinjyo I, Schambach F, Intlekofer AM, Banerjee A, Longworth SA, Vinup KE, Mrass P, Oliaro J, Killeen N, Orange JS, Russell SM, Weninger W, Reiner SL. Asymmetric T Lymphocyte Division in the Initiation of Adaptive Immune Responses. *Science*. 2007;315(5819):1687-1691. doi:10.1126/science.1139393

2. Jiang X, Clark RA, Liu L, Wagers AJ, Fuhlbrigge RC, Kupper TS. Skin infection generates non-migratory memory CD8+ TRM cells providing global skin immunity. *Nature*. 2012;483(7388):227-231. doi:10.1038/nature10851

3. Martin MD, Badovinac VP. Defining Memory CD8 T Cell. *Front Immunol*. 2018;9:2692. doi:10.3389/fimmu.2018.02692

4. Sallusto F, Lenig D, Förster R, Lipp M, Lanzavecchia A. Two subsets of memory T lymphocytes with distinct homing potentials and effector functions. *Nature*. 1999;401(6754):708-712. doi:10.1038/44385

5. Chang JT. Pathophysiology of Inflammatory Bowel Diseases. Longo DL, ed. *N Engl J Med*. 2020;383(27):2652-2664. doi:10.1056/NEJMra2002697

6. Ortega C, Fernández-A S, Carrillo JM, Romero P, Molina IJ, Moreno JC, Santamaría M. IL-17-producing CD8+ T lymphocytes from psoriasis skin plaques are cytotoxic effector cells that secrete Th17-related cytokines. *Journal of Leukocyte Biology*. 2009;86(2):435-443. doi:10.1189/JLB.0109046

7. Hassert M, Harty JT. Tissue resident memory T cells- A new benchmark for the induction of vaccine-induced mucosal immunity. *Front Immunol*. 2022;13:1039194. doi:10.3389/fimmu.2022.1039194

8. Gálvez-Cancino F, López E, Menares E, Díaz X, Flores C, Cáceres P, Hidalgo S, Chovar O, Alcántara-Hernández M, Borgna V, Varas-Godoy M, Salazar-Onfray F, Idoyaga J, Lladser A.Vaccination-induced skin-resident memory CD8 $^{+}$ T cells mediate strong protection against cutaneous melanoma. *OncoImmunology*. 2018;7(7):e1442163. doi:10.1080/2162402X.2018.1442163

9. Savas P, Virassamy B, Ye C, Salim A, Mintoff CP, Caramia F, Salgado R, Byrne DJ, Teo ZL, Dushyanthen S, Byrne A, Wein L, Luen SJ, Poliness C, Nightingale SS, Skandarajah AS, Gyorki DE, Thornton CM, Beavis PA, Fox SB, Darcy PK, Speed TP, Mackay LK, Neeson PJ, Loi, S. Single-cell profiling of breast cancer T cells reveals a tissue-resident memory subset associated with improved prognosis. *Nat Med*. 2018;24(7):986-993. doi:10.1038/s41591-018-0078-7

10. Ryan GE, Harris JE, Richmond JM. Resident Memory T Cells in Autoimmune Skin Diseases. *Front Immunol*. 2021;12:652191. doi:10.3389/fimmu.2021.652191

11. Milner JJ, Goldrath AW. Transcriptional programming of tissue-resident memory CD8+ T cells. *Current Opinion in Immunology*. 2018;51:162-169. doi:10.1016/j.coi.2018.03.017

12. Kok L, Masopust D, Schumacher TN. The precursors of CD8+ tissue resident memory T cells: from lymphoid organs to infected tissues. *Nat Rev Immunol*. 2022;22(5):283-293. doi:10.1038/s41577-021-00590-3

13. Kok L, Dijkgraaf FE, Urbanus J, Bresser K, Vredevoogd DW, Cardoso RF, Perié L, Beltman JB, Schumacher TN. A committed tissue-resident memory T cell precursor within the circulating CD8+ effector T cell pool. *Journal of Experimental Medicine*. 2020;217(10):e20191711. doi:10.1084/jem.20191711

14. Mora-Buch R, Bromley SK. Discipline in Stages: Regulating CD8+ Resident Memory T Cells. *Front Immunol*. 2021;11:624199. doi:10.3389/fimmu.2020.624199

15. Masopust D, Choo D, Vezys V, Wherry EJ, Duraiswamy J, Akondy R, Wang J, Casey KA, Barber DL, Kawamura KS, Fraser KA, Webby RJ, Brinkmann V, Butcher EC, Newell KA, Ahmed R. Dynamic T cell migration program provides resident memory within intestinal epithelium. *Journal of Experimental Medicine*. 2010;207(3):553-564. doi:10.1084/jem.20090858

16. Li G, Yang Q, Zhu Y, Wang HR, Chen X, Zhang X, Lu B. T-Bet and Eomes Regulate the Balance between the Effector/Central Memory T Cells versus Memory Stem Like T Cells. Matloubian M, ed. *PLoS ONE*. 2013;8(6):e67401. doi:10.1371/journal.pone.0067401

17. Mackay LK, Wynne-Jones E, Freestone D, Pellicci DG, Mielke LA, Newman DM, Braun A, Masson F, Kallies A, Belz GT, Carbone FR. T-box Transcription Factors Combine with the Cytokines TGF-β and IL-15 to Control Tissue-Resident Memory T Cell Fate. *Immunity*. 2015;43(6):1101-1111. doi:10.1016/j.immuni.2015.11.008

18. Hänninen A, Maksimow M, Alam C, Morgan DJ, Jalkanen S. Ly6C supports preferential homing of central memory CD8+ T cells into lymph nodes. *Eur J Immunol*. 2011;41(3):634-644. doi:10.1002/eji.201040760

19. Zhou X, Yu S, Zhao DM, Harty JT, Badovinac VP, Xue HH. Differentiation and Persistence of Memory CD8+ T Cells Depend on T Cell Factor 1. *Immunity*. 2010;33(2):229-240. doi:10.1016/j.immuni.2010.08.002

20. Jeannet G, Boudousquié C, Gardiol N, Kang J, Huelsken J, Held W. Essential role of the Wnt pathway effector Tcf-1 for the establishment of functional CD8 T cell memory. *Proc Natl Acad Sci USA*. 2010;107(21):9777-9782. doi:10.1073/pnas.0914127107

21. Wu J, Madi A, Mieg A, Hotz-Wagenblatt A, Weisshaar N, Ma S, Mohr K, Schlimbach T, Hering M, Borgers H, Cui, G. T Cell Factor 1 Suppresses CD103+ Lung Tissue-Resident Memory T Cell Development. *Cell Reports*. 2020;31(1):107484. doi:10.1016/j.celrep.2020.03.048

22. Escobar G, Mangani D, Anderson AC. T cell factor 1: A master regulator of the T cell response in disease. *Sci Immunol*. 2020;5(53):eabb9726. doi:10.1126/sciimmunol.abb9726

23. Sheridan BS, Pham QM, Lee YT, Cauley LS, Puddington L, Lefrançois L. Oral Infection Drives a Distinct Population of Intestinal Resident Memory CD8+ T Cells with Enhanced Protective Function. *Immunity*. 2014;40(5):747-757. doi:10.1016/j.immuni.2014.03.007

24. Laidlaw BJ, Zhang N, Marshall HD, Staron MM, Guan T, Hu Y, Cauley LS, Craft J, Kaech SM. CD4+ T Cell Help Guides Formation of CD103+ Lung-Resident Memory CD8+ T Cells during Influenza Viral Infection. *Immunity*. 2014;41(4):633-645. doi:10.1016/j.immuni.2014.09.007